Implementation of Piezoelectric (PZT) Sensors on the Boeing 737NG Aft Pressure Bulkhead Structure

JEONG-BEOM IHN, HANFEI MEI, JIM DUNNE, OHCHANG JIN, WALT JARECKI and ZEB TIDWELL

ABSTRACT

This paper summarizes the results of the validation testing conducted to support the development of piezoelectric (PZT) sensors for crack detection in the 737NG Aft Pressure Bulkhead (APB) web at the Y-chord. The objectives of the tests were to evaluate detection capability, durability and reliability of PZT sensors under various environments and temperatures. The test results herein were collected from Boeing Laboratory, the FAA Technical Center and Stanford University. The results contained in this document are for engineering development purposes.

INTRODUCTION

Most critical aircraft structure have inspections to ensure structural airworthiness, but some of those inspections have frequent intervals and are difficult to access for traditional nondestructive methods [1, 2]. The use of PZT sensors as a structural health monitoring (SHM) system is an effective technique to safely monitor defects and damages before they become detrimental and compromise aircraft safety [3].

Boeing has been involved in the development of PZT sensors for structural health monitoring for over 30 years [4-6]. They have developed a design framework to custom design piezoelectric-based smart sensor layers for a specific structure configuration/application and algorithms that automatically process sensor data and determine damage states or changes in structural integrity. The onboard smart sensor layers are installed during the regular maintenance cycle and can be interrogated during the flight or on-ground to collect the data and determine damage state.

Boeing developed a PZT solution on the web of the 737NG Aft Pressure Bulkhead (APB) as an alternative inspection to Service Bulletin (SB) 737-53A1248. This is a safety bulletin due to reported in-service cracks on the 737 classic models and is mandated by the FAA with an Airworthiness Directive (AD). This area has inspections that do not align with regular maintenance intervals. SB 737-53A1248 allows operators two inspection methods – low frequency eddy current (LFEC) from the aft side every 1,200 flight cycles or high frequency eddy current (HFEC) from the forward side every 3,800 flight cycles [7].

Jeong-Beom Ihn, Hanfei Mei, Jim Dunne, Ohchang Jin, Zeb Tidwell, Walt Jarecki, The Boeing Company, 929 Long Bridge Drive, Arlington, Virginia, 22202, U.S.A.

The aft inspections are difficult due to the small access space and the forward inspections require the removal of the aft galley. The proposed PZT option will demonstrate equivalency to LFEC and utilize the same inspection interval.

Boeing partnered with Acellent Technologies on the customized sensor design for the 737NG APB. Boeing partnered with Stanford University and the FAA Technical Center to perform tests in addition to tests at their own lab facilities.

This paper will present the work on probability of detection (PoD) testing of PZT sensors for crack detection of 737NG APB specimens. Boeing has completed all testing. The test results demonstrate the reliability and durability of the PZT sensor technology under representative operational environments.

TEST DESCRIPTION

Test Articles

All test articles were flat lap splice specimens with a thicker Y-chord (0.070 inch) and a thinner web (0.032 inch) assembled with rivets.

Figure 1 shows the specimen design for PoD testing.

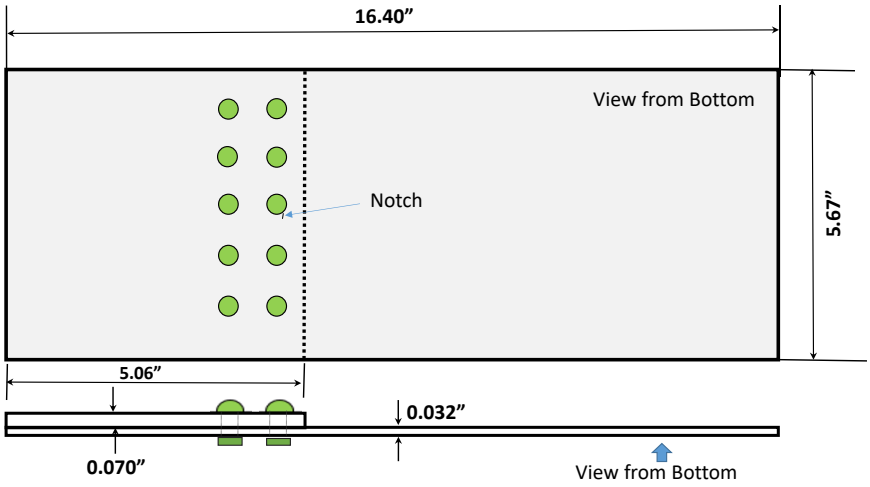

Figure 1: Schematic of PoD testing specimen configuration

Both Y-chord and bulkhead web were made from aluminum alloy 2024. An 0.05-inch-long × 0.005-inch-wide electro-discharging machine (EDM) notch was created on the web (see the location specified in Figure 1) before assembling the specimens. A total of twenty-four (24) specimens were fabricated with an EDM notch.

Sensor Installation

The PZT sensors manufactured by Acellent were installed at the Boeing Laboratory per the sensor installation procedure developed by Boeing.

Figure 2 shows the PZT sensors installed on the APB specimen. The sensor nodes should be located at mid-points between the rivets.

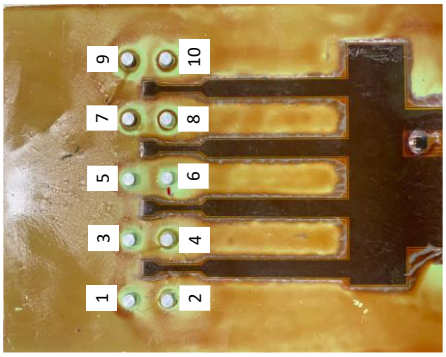

Figure 2: PZT sensors installed on PoD testing specimen

Fatigue test

Table 1 summarizes the parameters for PoD fatigue testing. The stress level (21 ksi) for PoD testing was determined based on engineering tests which showed that below 20 ksi the crack initiation from the EDM took more than 200,000 cycles.

Table 1: Fatigue test condition conditions

Test Type	Max stress (ksi)	Stress ratio	Frequency (Hz)
PoD	21	0.1	2~5

Figure 3 provides information on the nomenclature used to describe the crack as it grew. Each coupon started testing with an EDM notch that was 0.05" in length. As the coupon was fatigue cycled, a natural crack grew from the EDM notch. The length of the natural crack was designated the 'Delta' or 'Net' crack length. The net crack length is used throughout this paper.

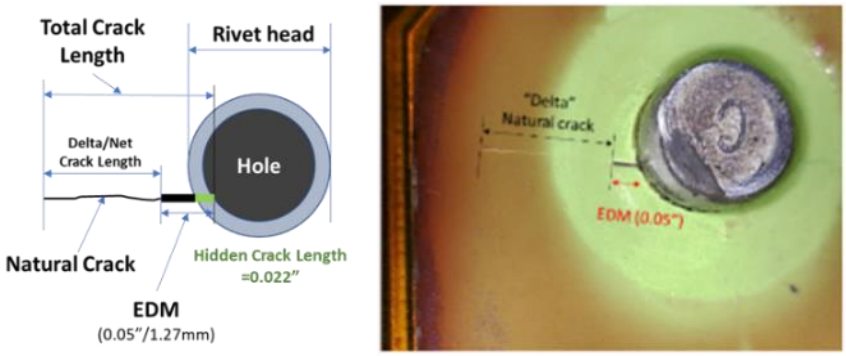

Figure 3: Illustration of the crack length nomenclature

Fatigue cycles, e.g., 5,000 cycles, were applied under load control and the PZT sensor readings were recorded using Acellent's ScanGenie system at ± 25 lbf. This

procedure was repeated three times, i.e., up to 15,000 fatigue cycles. These three measurements established the baseline sensor response. The fatigue cycling continued and was stopped periodically to determine crack initiation/growth from the EDM notch. When a crack was found, photos of the crack were taken to measure the crack length and the PZT sensor readings were recorded at -25°F, 0°F, 32°F, 100°F, 140°F and Room Temperature (RT) [8]. The minimum requirements for net crack sizes for the PZT sensor data collections were 1.0 mm (=0.039 in), 1.5 mm (=0.059 in), 2.0 mm (=0.079 in), 3.0 mm (=0.118 in), 4 mm (=0.157 in), 5.0 mm (=0.197 in) and 6.0 mm (=0.236 in). These are net crack growth from the EDM notch. The PoD testing was performed at Boeing, Stanford and FAA TC. An example (SN098012) of crack measurements with fatigue cycles is shown in Figure 4.

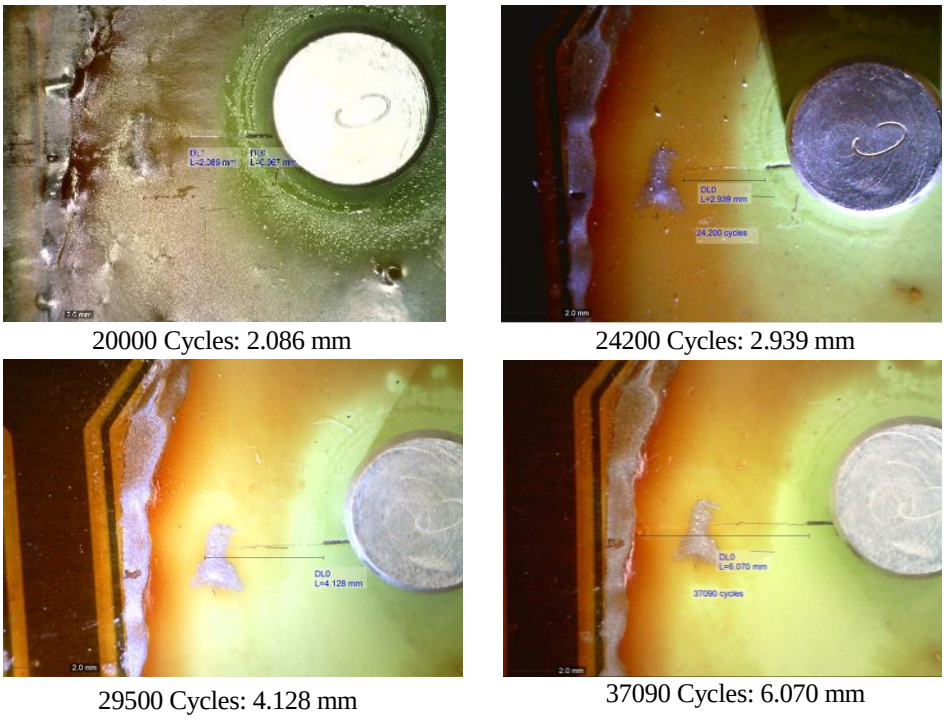

20000 Cycles: 2.086 mm

24200 Cycles: 2.939 mm

29500 Cycles: 4.128 mm

37090 Cycles: 6.070 mm

Figure 4: PoD crack length measurements for SN098012 at Rivet 6 (EDM notch)

DAMAGE ANALYSIS

A particular Damage Index (DI) used in Boeing proprietary damage analysis process is the drop in a correlation coefficient (DI7). This DI measures how well the two waveforms (baseline and current) within the analysis window are correlated with one another. The equation below defines how the DI is calculated (where x and y are the windowed baseline and current responses of a particular path). Two perfectly correlated waveforms will have a DI of zero whereas two uncorrelated waveforms will have a DI of 1. We can mathematically express the formula as:

$$DI7 = 1 - \frac{\frac{1}{n}\sum_{i=1}^{n}(x_i-\bar{x})(y_i-\bar{y})}{\sqrt{\frac{1}{n}\sum_{i=1}^{n}(x_i-\bar{x})^2\frac{1}{n}\sum_{i=1}^{n}(y_i-\bar{y})^2}} \quad (1)$$

where baseline data is x_i and test data is y_i.

Figure 5 show DI values for all potential PoD paths (short paths such as 2 to 7 have been found to be problematic due to crosstalk) from tests at Boeing. The DI7 results for paths that lead to Sensor 2 (left side of the hole with the EDM notch) show increasing DI as the crack grows. The DI7 results for paths that lead to Sensor 3 (right side of the same hole) show no change in DI values as the crack grows. Based on these results, three possible long paths were considered for the PoD analysis – the paths 12 to 2, 14 to 2 and 16 to 2 (only the even numbered transducers on the bottom row were considered since these are the likely production transducers). When evaluating DI7 values for these three closest paths the data in the plots above show that in general the path 14 to 2 is more sensitive to the crack growth. When looking at all coupons together it was observed that the path 14 to 2 has less zero-crack-length noise. Based on these two characteristics, the path 14 to 2 was selected for the PoD analysis.

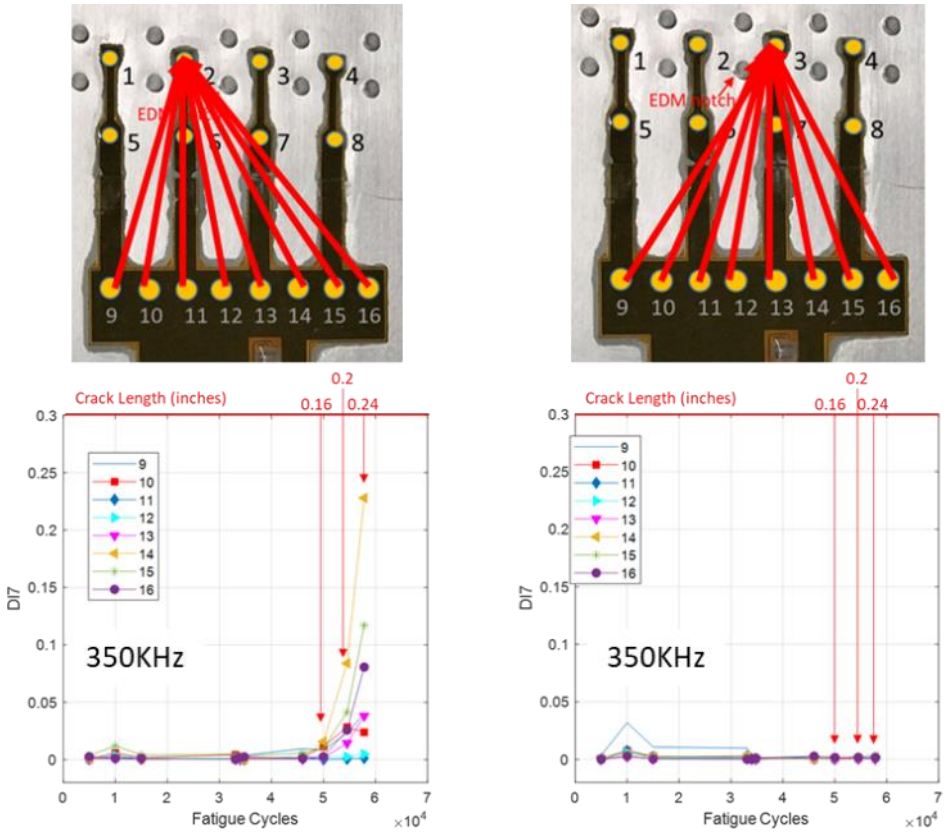

Figure 5: DI7 values for multiple paths tested at Boeing

POD RESULTS

Twenty-four (24) coupon data sets were used for the PoD analyses. First, the PZT signals from these coupons were collected at room temperature (RT) after several thousand cycles of fatigue testing. During the data collection, the PZT waveforms and crack lengths were recorded. These PZT waveforms were then converted to DI values. Figure 6 shows the DI and the net crack length for individual coupons.

Using these 125 values of DI and the smoothed density fit, the 99.9th percentile for DI is 0.00967. This implies that, based on the density, the probability of a DI being larger than 0.00967 for zero net crack length is 0.1%. This leads to a low chance of a noise from a no crack being called a crack. Based on this analysis, a DI threshold of 0.010 was used for PoD calculations. Note that the PoD curve is dependent on this threshold value. A lower threshold will lead to a lower a90/95 PoD value but a higher false call rate while a higher threshold will lead to a higher a90/95 PoD values and a lower false call rate. To estimate the PoD curve, Random Parameter Model (RPM) was used [9-11]. The PoD curve at RT is given in

Figure 7. Note that using 24 coupons and a DI threshold of 0.01, the a90 value is 0.183 inch and the a90/95 PoD is 0.193 inch.

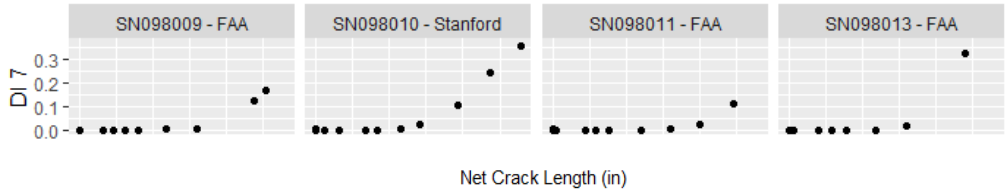

Figure 6: Representative DI values versus net crack lengths

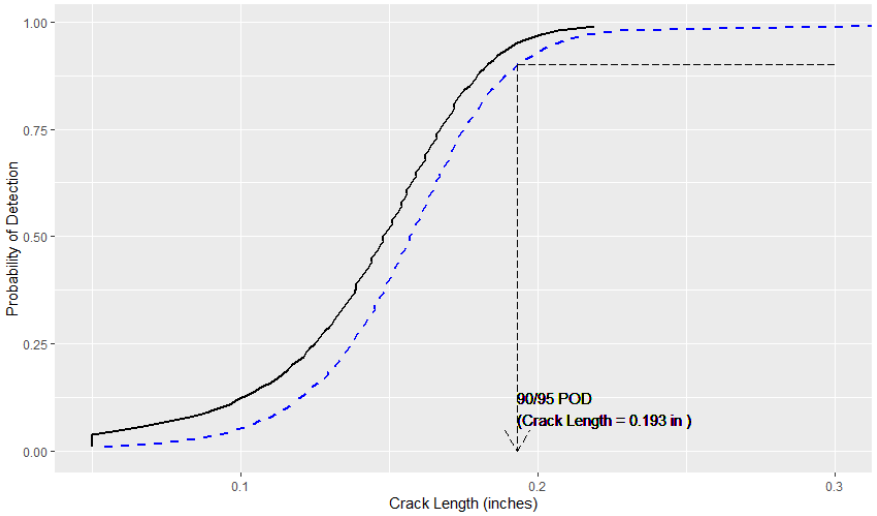

Figure 7: PoD estimated for data collected at Room Temperature. The solid black curve is the PoD curve, while the dashed blue curve is the 95% upper confidence bound of the PoD curve.

COMPARISON OF PODS AT DIFFERENT TEMPERATURES

DI information was calculated at low (32°F) and high (100°F) temperatures. PoDs from these data were also generated for comparison. The specific method used in the paper assumes that "targeted" temperatures (i.e., 32°F, 100°F) at baseline measurements are the same as "targeted" (i.e., 32°F, 100°F) temperatures at SHM measurements for DI calculations as a function of crack length. Any deviation of the true temperature from targeted temperatures would result in DI drifts and hence degrade the PoDs.

This led to a a90 value of 0.203 inches with a90/95 PoD of 0.220 inches for 32°F (Figure 8) and a a90 value of 0.184 inches with a90/95 PoD of 0.196 inches for 100°F (Figure 9). Note that the PoD from the 100°F data is similar to that from Room Temperature data. However, the PoD from the 32°F data was higher. This is an artifact of the threshold that was chosen. Note that at 32°F, the DI7 values for zero net crack had many values that were higher than those from RT or 100°F hence leading to a higher DI threshold used for PoD calculations.

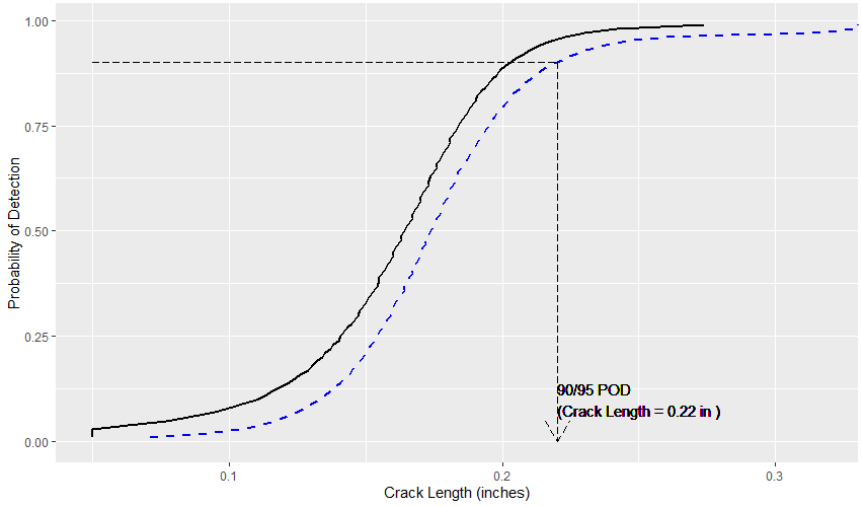

Figure 8: PoD estimates for data collected at 32°F. The solid black curve is the PoD curve, while the dashed blue curve is the 95% upper confidence bound of the PoD curve.

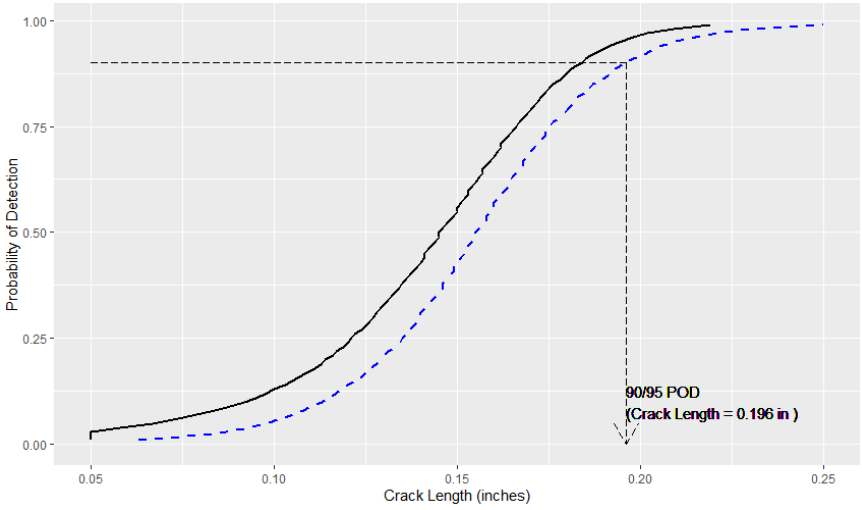

Figure 9: PoD estimates for data collected at 100oF. The solid black curve is the PoD curve, while the dashed blue curve is the 95% upper confidence bound of the PoD curve.

CONCLUSION

The a90/95 net crack length value at RT was calculated as 0.193 inches using the Random Parameter Model. PoD tests were conducted at -25°F, 0°F, 32°F, 100°F, 140°F

but the results discussed in this paper were for RT (71.9°F to 75.5°F), cold temperature (-0.5°F to 33.9°F) and elevated temperature (84.8°F to 112.1°F). Results from RT and 100 F were similar, while the 32°F led to a higher 90/95 PoD. Further PoD analysis via the same steps can be done to evaluate effects of -25°F, 0°F, 140°F data on PoD curves, which would then be able to establish an operation temperature limit for a PZT system.

ACKNOWLEDGMENTS

A special thanks goes to Amrita Kumar, Susheel Yadav, and Franklin Li from Acellent, Danielle Stephens and Paul Swindell from FAA, Pu Xie and Fu-Kuo Chang from Stanford University. They are all very dedicated for the advancement of Structural Health Monitoring and contributed to the success of this project.

REFERENCES

1. Piotrowski, D. (2024). Overview of SHM in airline maintenance: Challenges and opportunities. Structural Health Monitoring/Management (SHM) in Aerospace Structures, 3-14.
2. Tidwell, J. Z., & Jarecki, W. (2024). Boeing's Implementation of CVM sensors on the 737NG Aft Pressure Bulkhead. In AIAA SCITECH 2024 Forum (p. 2619).
3. Xie, P., Yadav, S. K., Ihn, J. B., Lee, B., Chang, F. K., & Tidwell, Z. (2025). Quantification of Lamb Wave-Based SHM Technique Through Ground Test Under Simulated Flight Environment for Commercial Airplane. In AIAA SCITECH 2025 Forum (p. 1222).
4. Ihn, J. B., Pado, L., Leonard, M., Desimio, M., & Olson, S. (2011). Development and Performance Quantification of an Ultrasonic Structural Health Monitoring System for Monitoring Fatigue Cracks on a Complex Aircraft Structure. Structural Health Monitoring 2011.
5. Pado, L. E., & Ihn, J. B. (2021). U.S. Patent No. 10,909,280. Washington, DC: U.S. Patent and Trademark Office.
6. Pado, L. E., Ihn, J. B., & Dunne, J. P. (2013). Understanding probability of detection (POD) in structure health monitoring systems. Structural Health Monitoring 2013.
7. SB 737-53A1248 Rev 2, "Fuselage - Body Station 1016 Aft Pressure Bulkhead Web - Inspection for Web Cracks at the Y-Chord", October 2015.
8. RTCA DO-160G, "Environmental Conditions and Test Procedures for Airborne Equipment", 2010, RTCA, INC.
9. O'Connor, E.L., Basu, S., Ihn, J.B., Pado, L., Dunne, J.P., "Study of Probability of Detection Estimation Methods for Structural Health Management," Boeing Technical Journal, vol. 12, no. 1, art. 6, 2022.
10. Neter, J., Kutner, M. H., Nachtsheim, C. J., & Wasserman, W. (1996). Applied linear statistical models.
11. Roach, D. P., Rice, T. M., & Swindell, P. (2017). Comparison of Multiple Statistical Methods for Calculating the Probability of Detection from SHM Systems (No. SAND2017-9630C). Sandia National Lab. (SNL-NM), Albuquerque, NM (United States).